

Update on a search for light NMSSM Higgs bosons in $H(125) \rightarrow \phi_1 \phi_1 \rightarrow 4\tau$ decays at $\sqrt{s}=13\text{TeV}$

Student: Dominik Wolfschläger

Supervisor: Alexei Raspereza

RWTH Aachen University

Introduction

The Next-to-Minimal Supersymmetric Standard Model (NMSSM) predicts the existence of two charged h^\pm , three CP-even - h_1, h_2, h_3 - and two CP-odd - a_1, a_2 - Higgs bosons [1]. In contrast to MSSM, the lightest bosons h_1 and a_1 can be much lighter than the discovered Higgs boson of mass 125 GeV, denoted $H(125)$ [2]. The $H(125)$ state can be either h_1 or h_2 and may decay into a pair of light bosons, $a_1 a_1$ or $h_1 h_1$. An update on a search for light NMSSM Higgs bosons produced in decays of the $H(125)$ state and decaying into τ leptons is presented. The analysis considered only gluon-gluon fusion (ggH) production of $H(125)$ so far. In this report we estimate the impact of the Vector Boson Fusion (VBF) process on the analysis sensitivity.

1 Signal topology

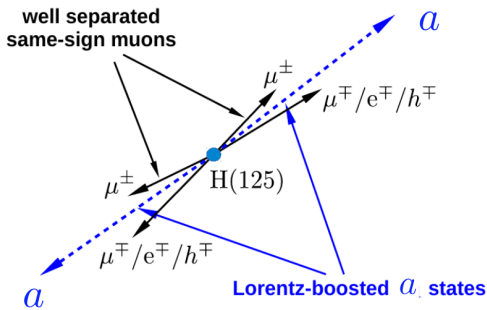


Fig. 1.1: Signal topology of the $H(125)$ decaying into two boosted ϕ_1 -bosons [3].

In this analysis a search for decays of $H(125)$ into two light ϕ_1 bosons, where ϕ_1 denotes either h_1 or a_1 , is performed. We investigate a mass range of $4 < m_{\phi_1} < 10$ GeV for which NMSSM predicts a sizeable branching fraction of $\phi_1 \rightarrow \tau\tau$ decays. The analysis selects final states in which one of the τ leptons in each ϕ_1 decay decays muonically and the other via 1-prong mode.

$$H(125) \rightarrow \phi_1 \phi_1 \rightarrow \tau_\mu \tau_{1\text{prong}} \tau_\mu \tau_{1\text{prong}}$$

This decay channel is depicted in figure 1.1. Due to their low mass compared to the $H(125)$ boson, the ϕ_1 bosons tend to be highly boosted and we expect the decay products of each ϕ_1 to be highly collimated and therefore have a small separation in the $\eta - \phi$ plane where η is pseudorapidity and ϕ the azimuthal angle. The signatures described above define the signal topology. The analysis targets events with two muons each accompanied by exactly one nearby charged particle.

1.1 Analysis strategy

The study is performed on proton-proton collision data collected with the CMS detector at $\sqrt{s} = 13$ TeV. The dataset corresponds to an integrated luminosity of 35.9fb^{-1} . A dedicated analysis has been developed to select events compatible with signal signatures. The selection criteria are presented in table 1.1. The main selection steps are discussed below.

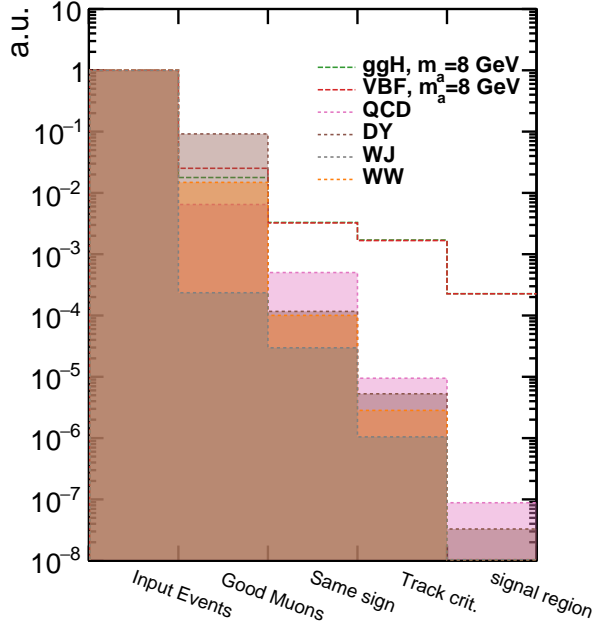


Fig. 1.2: Fraction of accepted events after each selection process in this analysis.

- **Muon selection:**

In the first step muons are selected which have a high transverse momentum and are reconstructed within the tracker acceptance. In order to reject heavy flavour hadron decays into muons the transverse impact parameter of the muon with respect to the primary interaction vertex d_{xy} must be smaller than 0.5 mm and the longitudinal impact parameter d_z must be smaller than 1 mm.

- **Muon pair selection:**

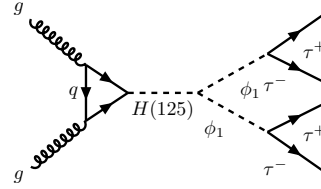
Muons are sorted by their p_T . An event is selected if it contains two muons with the same charge. This requirement almost entirely eliminates Drell-Yan, di-boson and $t\bar{t}$ backgrounds and significantly reduces QCD multi-jet background. In addition, two muons are required to be separated by $\Delta R > 2$ in $\eta - \phi$ plane. Figure 1.5 shows distributions of transverse momenta and pseudorapidities of leading and trailing muons after selection of same-sign muon pairs. Good agreement between data and simulation is observed.

- **Track+Muon selection:**

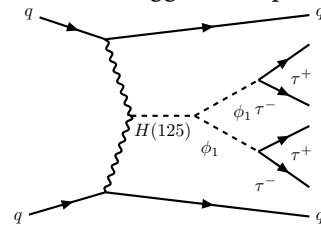
Each muon must be accompanied by exactly one charged particle within the isolation cone of $\Delta R < 0.5$ around the muon momentum. The charge of the particle must be opposite to the charge of the muon due to charge conservation in the decay of the neutral ϕ_1 state. The tracks accompanying muons must have impact parameters $|d_{xy}| < 0.2$ mm and $|d_z| < 0.4$ mm.

The selection criteria outlined above define the signal region. Figure 1.2 shows the reduction of background and signal efficiency after each step of the selection. The total number of selected data events, the expected background yields and the expected signal yields are presented in table 1.2. The expected signal yields are obtained assuming the standard model cross sections $\sigma_{ggH} = 43.92$ pb and $\sigma_{VBF} = 3.748$ pb and a benchmark branching fraction of $\mathcal{B}(H(125) \rightarrow \phi_1 \phi_1) \cdot \mathcal{B}^2(\phi \rightarrow \tau\tau) = 20\%$ [4].

2 Impact of VBF production on the analysis sensitivity



a) Gluon fusion Higgs boson production.



b) Vector boson fusion Higgs production.

Fig. 1.3: Feynman diagrams of the two relevant Higgs production mechanisms considered in this analysis.

Table 1.1: Overview of applied cuts for the signal extraction.

Analysis step	Cut	value
Good muon selection	Muon high p_T/η	$p_T < 18 \text{ GeV}, \eta < 2.4$
	Muon low p_T/η	$p_T < 9 \text{ GeV}, \eta < 2.4$
	Muon IP	$ d_{xy} < 0.5 \text{ mm}, d_z < 1 \text{ mm}$
Muon pair selection	Same sign muon pair	$q_{\mu_1} \cdot q_{\mu_1} = +1$
	Separation of μ tracks	$\Delta R(\mu_1, \mu_2) > 2$
Track+Muon selection	Track p_T/η	$p_T < 2.5 \text{ GeV}, \eta < 2.4$
	Track IP	$ d_{xy} < 0.2 \text{ mm}, d_z < 0.4 \text{ mm}$
	Track charge	$q_\mu \cdot q_{\text{trk}} = -1$
	Separation μ -track	$\Delta R(\mu_1, \text{trk}) < 0.5$
Signal region	#LeadingMuon/LeadingTrack	1
	#TrailingMuon/TrailingTrack	1

Figure 1.3 shows the feynman diagrams of the signal processes considered in this analysis. Up to now, this analysis considered only the ggH process which has the largest cross section among all Higgs boson production mechanisms. In this report we investigate the impact of the VBF process on the analysis sensitivity.

2.1 Higgs p_T reweighting

There are several Monte Carlo generators available to simulate Standard model and SUSY processes. Samples of $H(125) \rightarrow \phi_1 \phi_1 \rightarrow 4\tau$ were obtained for masses between 4 and 10 GeV using leading-order event generator PYTHIA 8 [5]. To account for higher order corrections the Higgs p_T spectrum has been reweighted with k-factors obtained with the next-to-leading-order event generator Powheg [6]. The p_T spectra of both samples are shown in the top plot of figure 1.4. The k-factors are obtained by dividing the normalised distributions obtained with PYTHIA 8 and Powheg event generators. They are shown in the lower plot of figure 1.4.

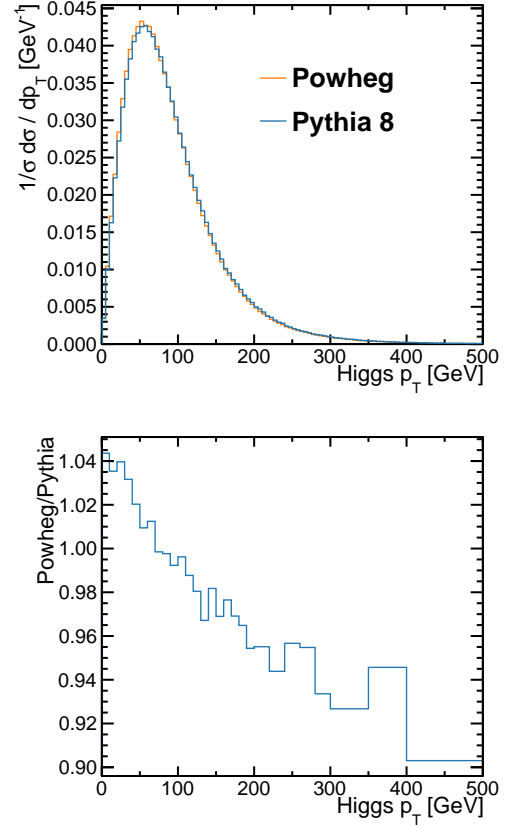


Fig. 1.4: Top plot: Transverse momentum p_T of the H (125) Higgs boson for both Powheg and PYTHIA 8 samples. Bottom plot: k-factor as a function Higgs p_T for reweighting the PYTHIA 8 samples.

Table 1.2: Yields after final selection for data, background and signal.

Process	yield ggH		yield VBF	
EWK	26.8 \pm	19.4		
$t\bar{t}$ +jets	18.8 \pm	2.5		
QCD	2033.3 \pm	673.8		
Data	2035			
$m_{\phi_1} = 4$ GeV	125.8 \pm	6.6	8.4 \pm	0.2
$m_{\phi_1} = 5$ GeV	90.8 \pm	5.5	6.9 \pm	0.2
$m_{\phi_1} = 6$ GeV	103.2 \pm	6.0	7.5 \pm	0.2
$m_{\phi_1} = 7$ GeV	103.2 \pm	5.7	7.5 \pm	0.1
$m_{\phi_1} = 8$ GeV	71.6 \pm	5.0	6.1 \pm	0.1
$m_{\phi_1} = 9$ GeV	70.5 \pm	5.0	4.2 \pm	0.1
$m_{\phi_1} = 10$ GeV	56.4 \pm	4.4	2.7 \pm	0.1

2.2 Signal extraction

The signal is extracted by applying a Maximum Likelihood Fit to the 2D distribution of the invariant mass of the muon-track pairs. The fit is performed with the superposition of signal and background templates. The normalisations of both signal and background templates are allowed to float freely in the fit. The signal templates are constructed using simulated Monte Carlo samples. Plots comparing the shapes of the muon-track invariant mass between ggH and VBF signal samples for three representative masses are shown in figure 1.6. The shapes of both production mechanisms are very similar which allows to construct a resulting signal template by adding up ggH and VBF templates.

The 2D background model of the invariant mass of the muon-track pairs is constructed using the following formula

$$f_{2D}(m_1, m_2) = C(m_1, m_2) \cdot (f_{1D}(m_1) \cdot f_{1D}(m_2)),$$

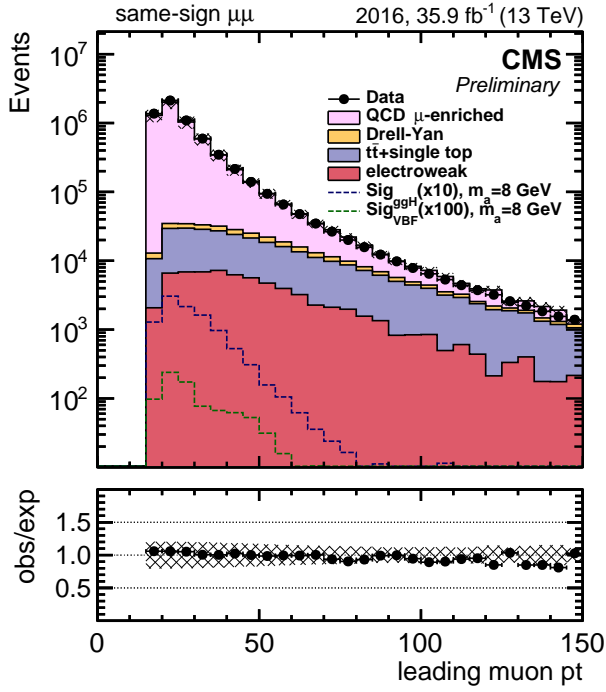
where f_{1D} is the 1D invariant mass distribution of one muon-track pair and $C(m_1, m_2)$ are mass correlation coefficients. Both f_{1D} and $C(m_1, m_2)$ are derived from the sideband region where one or both muons have more than one accompanying track. The muon-track invariant masses are ordered and filled into a binned 2D template.

The binning of the 2D distribution is illustrated in figure 1.7. Since the muon-track invariant masses are ordered the total number of independent bins is 21. Figure 1.8 shows the 1D distributions for three representative signal samples and for the background model derived from the sideband region. The figure 1.9 shows the correlation coefficients $C(m_1, m_2)$ computed from the sideband region. The signal is extracted with the unrolled 2D distribution shown in figure 1.10. The distribution in data is not shown as the analysis is still kept blinded. The unrolled 2D background template is normalised to the total data yield after the final selection.

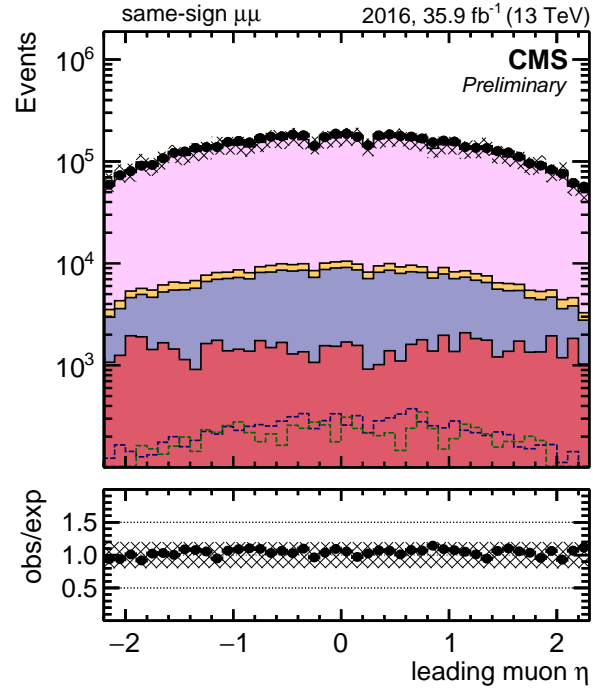
Expected limits

The analysis sensitivity is estimated in terms of expected limits on the branching ratio $\mathcal{B}(H(125) \rightarrow \phi_1 \phi_1) \cdot \mathcal{B}^2(\phi \rightarrow \tau\tau)$ assuming Standard model cross sections for ggH and VBF production modes. The modified frequentist CLs criterion, implemented in the ROOSTATS [7] package, is used for the calculation of the exclusion limits. In the process of limit setting the following systematic uncertainties are taken into account [3].

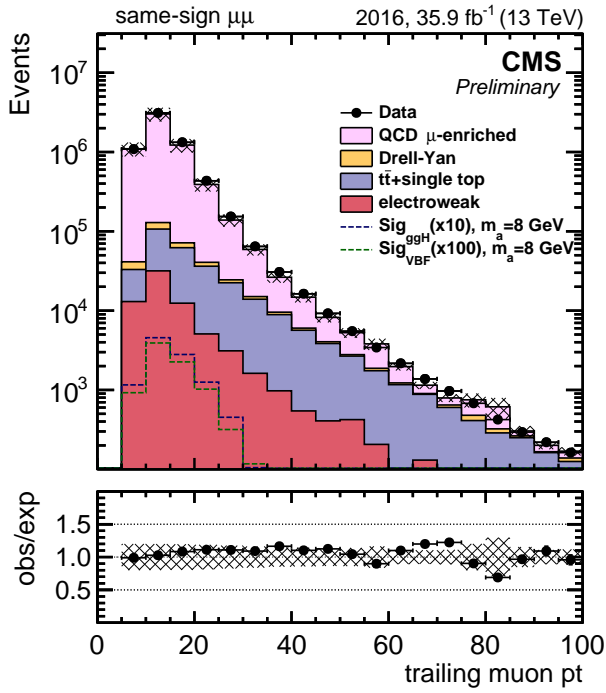
- The uncertainty in the **integrated luminosity** is estimated to be 2.6%.



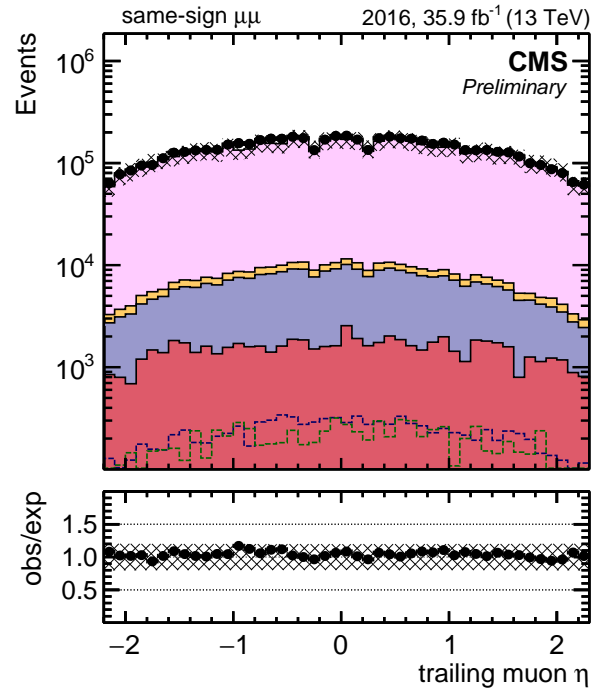
a) p_T distribution of leading muons.



b) η distribution of leading muons.



c) p_T distribution of trailing muons.



d) η distribution of trailing muons.

Fig. 1.5: Control plots of the p_T and η distributions of muon pairs selected during the muon pair selection of the signal extraction. Both ggH signal (blue) and VBF signal (green) are shown scaled by a factor of 10 and 100 respectively.

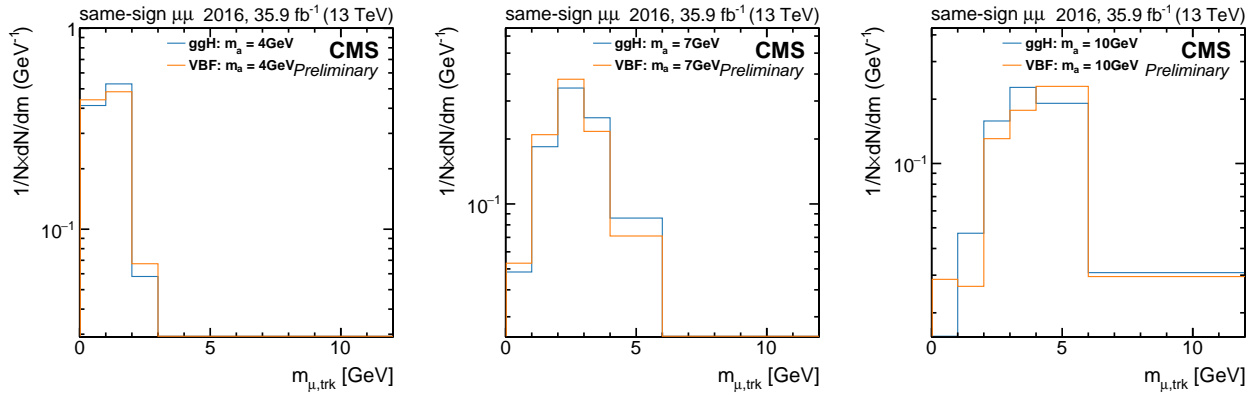


Fig. 1.6: Normalised distributions of the invariant mass of the selected muon-track pairs for masses of 4,7 and 10GeV.

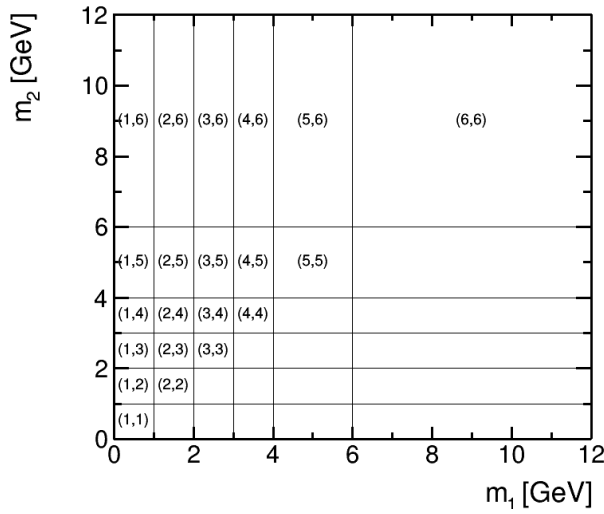


Fig. 1.7: Binned template of the correlation coefficients $C(i,j)$.

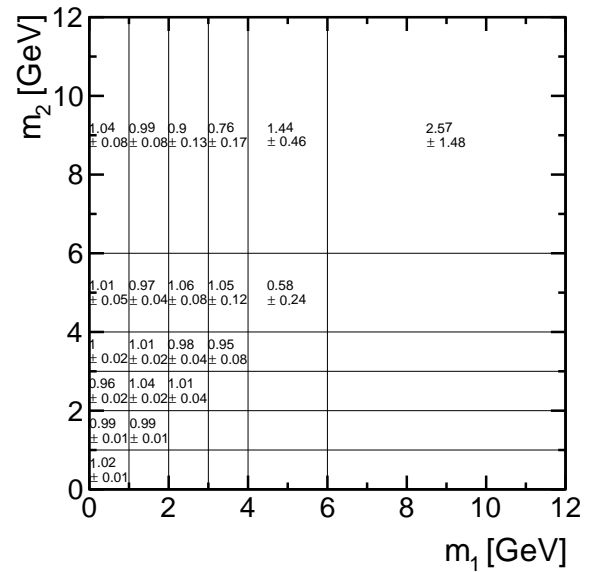


Fig. 1.8: Mass correlation coefficients $C(i,j)$ evaluated from the sideband region with statistical uncertainties.

- The **muon identification and trigger efficiency** uncertainty is assumed to be 2% per muon.
- An uncertainty of 5% in the **track selection and isolation efficiency** is assigned for each track.
- **MC statistical uncertainties** range from 7 to 100%.
- statistical uncertainties in the **correlation coefficients** in the background model range from 1 to 70%.

In left plot of figure 1.11 the expected limit on the branching fraction is shown when only ggH production mechanism is considered. In the right plot expected limits are computed when ggH and VBF production processes are taken into account. In the second case the limit ranges from 3.3% at $m_{\phi_1} = 9$ GeV to 25.5% at $m_{\phi_1} = 5$ GeV.

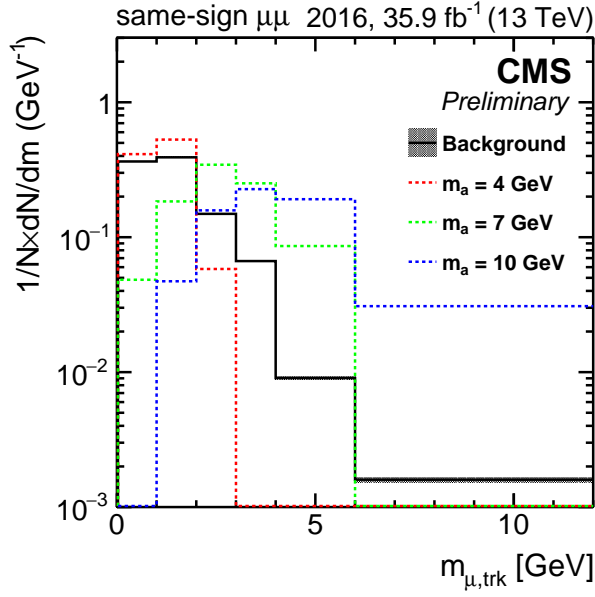


Fig. 1.9: 1D distribution of background and three representative signal samples.

Table 1.3: Ratio of old limit compared to the updated limit.

Ratio of exp. limits	exp
$m_{\phi_1} = 4 \text{ GeV}$	1.049
$m_{\phi_1} = 5 \text{ GeV}$	1.063
$m_{\phi_1} = 6 \text{ GeV}$	1.078
$m_{\phi_1} = 7 \text{ GeV}$	1.046
$m_{\phi_1} = 8 \text{ GeV}$	1.089
$m_{\phi_1} = 9 \text{ GeV}$	1.061
$m_{\phi_1} = 10 \text{ GeV}$	1.053

Table 1.3 presents a ratio of the expected limits computed without and with inclusion of VBF samples. Inclusion of the VBF samples improves limits by 5-9% depending on m_{ϕ_1} which is consistent with the ratio of VBF and ggH production rates.

3 Conclusion

A search for very light NMSSM Higgs bosons in the decay $H(125) \rightarrow 2\phi_1 \rightarrow 4\tau$ is updated. Masses in the range of $4 < m_{\phi_1} < 10 \text{ GeV}$ are probed. The contribution from VBF is included in the signal model. This reduces the expected limit on the branching fraction by 5% to 9% relative to the limit expected when only ggH process is taken into account. In a next step the impact of Higgs-strahlung process on the analysis sensitivity can be studied once the necessary Monte Carlo samples become available.

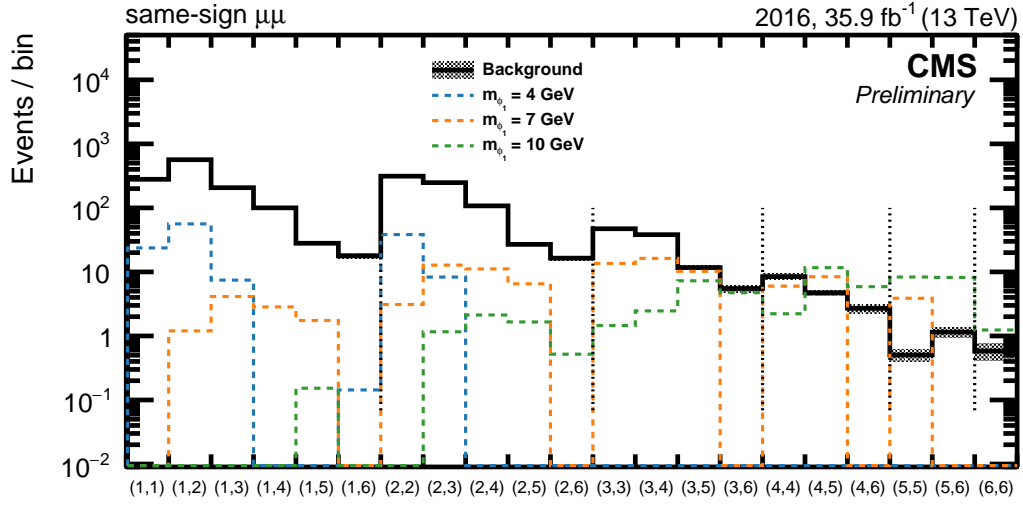
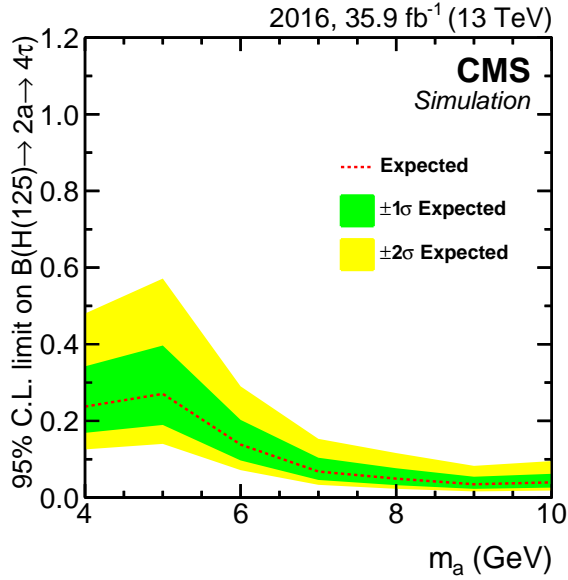
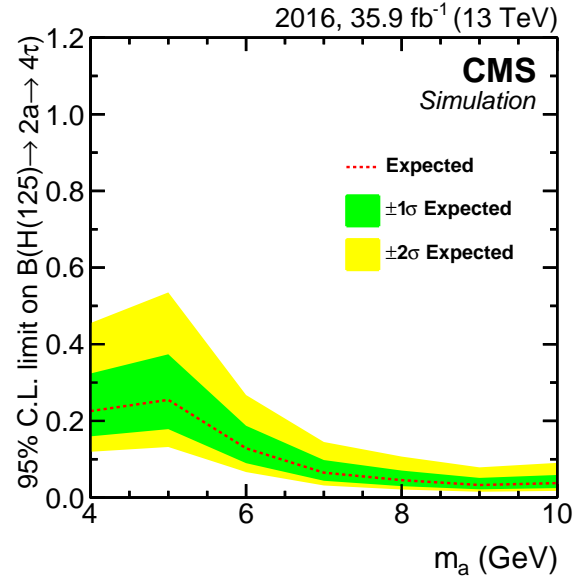


Fig. 1.10: Unrolled 2D distribution used for the signal extraction. The bin labeling follows the definition in figure 1.7.



a) ggH samples only.



b) ggH+VBF samples.

Fig. 1.11: Expected limit for on the branching ratio of the $H(125) \rightarrow 2\phi_1 \rightarrow 4\tau$ decay.

Bibliography

- [1] Ulrich Ellwanger, Cyril Hugonie, and Ana M. Teixeira. “The Next-to-Minimal Supersymmetric Standard Model”. In: *Phys.Rept.* 496:1-77,2010 (Oct. 9, 2009). arXiv: 0910.1785v5 [hep-ph] (cit. on p. 1).
- [2] The CMS Collaboration. “Observation of a new boson at a mass of 125 GeV with the CMS experiment at the LHC”. In: *Phys. Lett. B* 716 (2012) 30 (July 31, 2012). arXiv: 1207.7235v2 [hep-ex] (cit. on p. 1).
- [3] CMS Collaboration. “Search for a very light NMSSM Higgs boson produced in decays of the 125 GeV scalar boson and decaying into tau leptons in pp collisions at $\sqrt{s} = 8$ TeV”. In: *JHEP* 01 (2016) 079 (Oct. 22, 2015). arXiv: 1510.06534v2 [hep-ex] (cit. on pp. 1, 4).
- [4] A. Raspereza S. Consuegra Rodriguez. “NMSSM $H(125) \rightarrow aa \rightarrow 4\tau$ Search with 2016 Dataset”. In: (June 26, 2017) (cit. on p. 2).
- [5] Torbjörn Sjöstrand, Stephen Mrenna, and Peter Skands. “A Brief Introduction to PYTHIA 8.1”. In: *Comput.Phys.Commun.* 178:852-867,2008 (Oct. 20, 2007). arXiv: 0710.3820v1 [hep-ph] (cit. on p. 3).
- [6] Carlo Oleari. “The POWHEG-BOX”. In: *Nucl.Phys.Proc.Suppl.* 205-206:36-41,2010 (July 22, 2010). arXiv: 1007.3893v1 [hep-ph] (cit. on p. 3).
- [7] Lorenzo Moneta, Kevin Belasco, Kyle Cranmer, et al. “The RooStats Project”. In: (Sept. 6, 2010). arXiv: 1009.1003v2 [physics.data-an] (cit. on p. 4).